

# General Solutions for Tunneling of Scalar Fields with Quartic Potentials in de Sitter Space

Misao Sasaki, Ewan D. Stewart and Takahiro Tanaka  
Department of Physics  
Kyoto University  
Kyoto 606, Japan

April 26, 2024

## Abstract

The tunneling rates for scalar fields with quartic potentials in de Sitter space in the limit of no gravitational back reaction are calculated numerically and the results are fitted by analytic formulae.

# 1 Introduction

The decay of a false vacuum and/or creation of topological defects through quantum tunneling in the early Universe may play an important role in determining the subsequent structure of the Universe. These phenomena are particularly important in the context of inflationary cosmology. The nucleation of true vacuum bubbles associated with false vacuum decay is incorporated in several viable models of inflation as a mechanism to terminate the inflationary expansion of the Universe [1]. Quantities such as the efficiency of thermalization by bubble collisions or the degree of spatial inhomogeneities crucially depend on the nucleation rate. Also, topological defects such as domain walls, strings, or monopoles may be created during the inflationary stage of the Universe [2]. In order to quantify their effects on the structure of the Universe, it is necessary to know their formation rates.

The study of false vacuum decay was initiated by Voloshin, Kobzarev, and Okun [3], and subsequently developed by Coleman [4], who showed how to calculate the tunneling rate by applying the instanton method to a scalar field having two nondegenerate minima. According to this method, the nucleation rate is crucially determined by the value of the action of a nontrivial classical Euclidean solution having  $O(4)$  symmetry, called the bounce solution. Coleman also argued that the formation and evolution of the true vacuum bubble are described by the analytic continuation of the bounce solution to Lorentzian time. Then Coleman and De Luccia [5] made an attempt to include gravitational effects in the bounce and obtained several important new results. However, their explicit results assume the thin-wall approximation, under which the space outside the bubble wall is exactly in the false vacuum. Hence it was unnecessary to know the behavior of the bounce solution there.

Once the thin-wall approximation is relaxed, it becomes indispensable to consider the global structure of the bounce solution. In particular, when the Euclidean Einstein equations are solved simultaneously, a finite vacuum energy density in the false vacuum inevitably gives the topological structure of  $S^4$  for the bounce solution, leading to the absence of the asymptotic infinity in the Euclidean space. Subsequent studies by various people have shown that this fact can cause very different behavior of the bounce solution compared with the case of a flat Euclidean background. For example, in the other extreme limit in which the width of the bubble wall would be very large, the solution reduces to a perfectly homogeneous  $S^4$  with the value of the scalar field staying at the top of the potential barrier. This is known as the Hawking-Moss solution [6]. Another interesting case is that of a potential with degenerate minima. A bounce solution with finite action exists in this case because of the compactness of the four-volume, contrary to the case of a flat Euclidean background. This describes the formation of a topological defect (a domain wall in the case of a single real scalar field) [2].

In the thin-wall and Hawking-Moss limits one can evaluate the bounce action

analytically. However, for intermediate cases it must be evaluated numerically. Thus, considering the important role played by the bounce action, it is desirable and useful to have a formula to evaluate the general bounce action ready to our hands.

In this paper, we consider a real scalar field with a general quartic potential, and evaluate numerically the bounce action by varying the parameters. Then, using the results, we construct fitting formulae which can be applied to wide ranges of the parameter space. This is a generalisation of the procedure of Ref. [7] which was only valid in the flat space limit. In Section 2 we introduce the formalism and derive our basic equations. In Section 3 we derive analytic results for the Hawking-Moss and thin-wall limits. In Section 4 we present our numerical results and various analytic fitting formulae.

## 2 Method

### 2.1 General tunneling formalism

Following the prescription given by Coleman and De Luccia [5], the tunneling rate in de Sitter space in the semiclassical limit is given by

$$\Gamma \propto e^{-B/\hbar}, \quad (1)$$

where  $B$  is the bounce action. It is defined to be

$$B = S_E[\phi_I(\mathbf{x}, \tau)] - S_E[\phi_0], \quad (2)$$

where  $S_E$  is the Euclidean action,  $\tau = it$  is the Euclidean time,  $\phi_0$  is the false vacuum value of the scalar field, and  $\phi_I(\mathbf{x}, \tau)$  is the instanton [8] with minimum Euclidean action. An instanton is a solution of the Euclidean equations of motion which interpolates from one side of the potential barrier to the other.<sup>1</sup> The instanton with minimum Euclidean action will dominate the tunneling rate. It corresponds to the lowest saddle point in the Euclidean action, whose single negative mode interpolates between the false and true vacuum states. In flat space it can be proved that the instanton has  $O(4)$  symmetry [9] and it is usually assumed that this is also the case in de Sitter space [5]. The Euclidean action for a scalar field minimally coupled to gravity is

$$S_E = \int d^4x \sqrt{g} \left[ -\frac{1}{16\pi G} R + \frac{1}{2} g^{\mu\nu} \partial_\mu \phi \partial_\nu \phi + V(\phi) \right]. \quad (3)$$

Assuming  $O(4)$  symmetry gives

$$ds^2 = d\xi^2 + a^2(\xi) d\Omega^2, \quad \phi = \phi(\xi), \quad (4)$$

---

<sup>1</sup>The Hawking-Moss instanton is the degenerate case of this in that it sits on top of the potential barrier.

and

$$S_E = 2\pi^2 \int d\xi \left\{ -\frac{3}{8\pi G} a (\dot{a}^2 + 1) + a^3 \left[ \frac{1}{2} \dot{\phi}^2 + V(\phi) \right] \right\}. \quad (5)$$

## 2.2 A quartic potential

In this paper we limit ourselves to the case of a quartic potential with a local minimum (the false vacuum) at  $\phi = 0$ , a local maximum (the top of the potential barrier) at  $\phi = \phi_+$ , and a global minimum (the true vacuum) at  $\phi = \phi_-$ . The potential can be written as

$$V(\phi) = V_0 + \frac{1}{2} m^2 \phi^2 - \mu \phi^3 + \lambda \phi^4. \quad (6)$$

Using the following change of variables we can eliminate two of the five parameters from the dynamics:

$$\psi = \frac{\mu}{m^2} \phi, \quad \rho = ma, \quad \zeta = m\xi, \quad (7)$$

$$H_0 = \frac{1}{m} \sqrt{\frac{8\pi G V_0}{3}}, \quad \nu = \frac{2\lambda m^2}{\mu^2}, \quad (8)$$

and

$$\kappa = \frac{8\pi G m^4}{\mu^2} = \frac{8\pi}{m_{\text{Pl}}^2} \frac{m^4}{\mu^2}. \quad (9)$$

It will also be useful to introduce the notation

$$\varepsilon = 1 - \nu. \quad (10)$$

Then

$$S_E = \frac{2\pi^2 m^2}{\mu^2} \int d\zeta \left\{ -\frac{3}{\kappa} \rho (\dot{\rho}^2 + 1 - H_0^2 \rho^2) + \rho^3 \left[ \frac{1}{2} \dot{\psi}^2 + U(\psi) \right] \right\}, \quad (11)$$

where

$$U(\psi) = \frac{1}{2} \psi^2 - \psi^3 + \frac{1}{2} \nu \psi^4. \quad (12)$$

The Euclidean equations of motion are

$$\ddot{\psi} + 3 \frac{\dot{\rho}}{\rho} \dot{\psi} = U', \quad (13)$$

$$\dot{\rho}^2 - 1 + H_0^2 \rho^2 = \frac{\kappa}{3} \rho^2 \left( \frac{1}{2} \dot{\psi}^2 - U \right), \quad (14)$$

and the bounce action is

$$B = S_E[\psi(\zeta), \rho(\zeta)] - S_E \left[ 0, \frac{1}{H_0} \sin H_0 \zeta \right]. \quad (15)$$

Note that  $U(\psi)$  has its local maximum and global minimum at

$$\psi_{\pm} = \frac{3}{4\nu} \left( 1 \mp \sqrt{1 - \frac{8}{9}\nu} \right), \quad (16)$$

respectively, and  $U(\psi_-) = 0$  when  $\nu = 1$  so that  $0 \leq \nu \leq 1$ .

### 2.3 Gravitational back reaction

The gravitational back reaction will be negligible if  $\kappa \ll 1$  except for in the thin-wall limit,  $\varepsilon \ll 1$  and  $H_0 \ll 1$  (see Section 3.2). The bounce action for a general potential in the thin-wall limit has been given in Ref. [10], and in our case it reduces to

$$B = \frac{m^2 \pi^2}{\mu^2} \frac{1}{3 \sqrt{\left(\varepsilon - \frac{1}{24}\kappa\right)^2 + H_0^2} \left[ \left(\varepsilon + \sqrt{\left(\varepsilon - \frac{1}{24}\kappa\right)^2 + H_0^2}\right)^2 - \left(\frac{1}{24}\kappa\right)^2 \right]}. \quad (17)$$

We see that the gravitational back reaction is negligible for  $\kappa \ll H_0$  or  $\kappa \ll \varepsilon$ . Thus for  $\kappa \ll \min\{1, \max\{H_0, \varepsilon\}\}$  the gravitational back reaction is negligible and we will assume this throughout the rest of the paper. The Euclidean equations of motion then become

$$\rho = \frac{1}{H_0} \sin H_0 \zeta, \quad (18)$$

and

$$\ddot{\psi} + 3H_0 \cot H_0 \zeta \dot{\psi} = U', \quad (19)$$

and the bounce action becomes

$$B = \frac{m^2}{\mu^2} \frac{2\pi^2}{H_0^3} \int_0^{\frac{\pi}{H_0}} d\zeta \sin^3 H_0 \zeta \left[ \frac{1}{2} \dot{\psi}^2 + U(\psi) \right]. \quad (20)$$

The dynamics now depends on only two parameters,  $\nu$  and  $H_0$ , and so a numerical treatment becomes tractable. See Figure 1 for a description of the parameter space and a sketch of our results.

## 3 Analytic Results

### 3.1 The Hawking-Moss instanton

The Euclidean equation of motion, Eq. (19), always has the trivial solution  $\psi = \psi_+$ . This is called the Hawking-Moss instanton. In flat space it has infinite

bounce action and plays no role, but because Euclidean de Sitter space has a finite volume,  $8\pi^2/3H^4$ , it has a finite bounce action

$$B = \frac{m^2}{\mu^2} \frac{8\pi^2}{3H_0^4} U(\psi_+) \quad (21)$$

in de Sitter space and is the dominant instanton for sufficiently large  $H_0$ . For our simple case of a quartic potential the condition under which the Hawking-Moss instanton dominates can be obtained by the perturbative analysis below [11], but for a general potential this will not be valid because the bounce action depends on the global properties of the potential and not just on the local properties around the top of the potential barrier.

Let  $\omega^2 \equiv -U''(\psi_+) = 2 - 3\psi_+$  and  $\chi = \psi - \psi_+$ . Assume  $\chi \ll 1$ . Then, from Eq. (19),

$$\ddot{\chi} + 3H_0 \cot H_0\zeta \dot{\chi} + \omega^2\chi \simeq 0. \quad (22)$$

This equation has a nontrivial regular solution only for  $\omega^2 = n(n+3)H_0^2$  where  $n = 0, 1, 2, \dots$ . For  $\omega = 0$  it is  $\chi = \text{constant}$ . For  $\omega \ll H_0$ , we expect it still to be an approximate solution, in which case  $B$  is maximised for  $\chi = 0$ . Note that we must maximise  $B$  to obtain a solution that interpolates from one side of the potential barrier to the other. For  $\omega = 2H_0$  the regular solution is

$$\chi = A \cos H_0\zeta, \quad (23)$$

and for  $\omega \simeq 2H_0$  we expect it still to be an approximate solution. Then for  $A$  sufficiently small,  $A^2 \ll \omega^2 - 4H_0^2$ ,

$$B = \frac{m^2}{\mu^2} \frac{8\pi^2}{3H_0^4} \left\{ U(\psi_+) - \frac{1}{10} (\omega^2 - 4H_0^2) A^2 \right\}. \quad (24)$$

Therefore for  $\omega^2 < 4H_0^2$ ,  $B$  is minimised for  $A = 0$ , i.e., the Hawking-Moss instanton; while for  $\omega^2 > 4H_0^2$ ,  $B$  is minimised for  $A \rightarrow \infty$ , i.e., the Hawking-Moss instanton is no longer the dominant instanton. Thus the Hawking-Moss instanton dominates for

$$H_0^2 \geq \frac{1}{2} \left( 1 - \frac{3}{2}\psi_+ \right). \quad (25)$$

Now we will calculate the first-order corrections to Eq. (21) for  $0 < \omega^2 - 4H_0^2 \ll 1$ . From Eqs. (12) and (19),

$$\ddot{\chi} + 3H_0 \cot H_0\zeta \dot{\chi} + 4H_0^2\chi = -(\omega^2 - 4H_0^2)\chi - 3(1 - 2\nu\psi_+)\chi^2 + 2\nu\chi^3. \quad (26)$$

This has the approximate solution [12]

$$\chi = A \cos H_0\zeta + \frac{1 - 2\nu\psi_+}{2 - 3\psi_+} A^2 \cos 2H_0\zeta + O(A^3 \cos 3H_0\zeta), \quad (27)$$

where

$$A^2 = \frac{7(2-3\psi_+)}{6(1-\nu\psi_+)} (\omega^2 - 4H_0^2) + O\left((\omega^2 - 4H_0^2)^2\right). \quad (28)$$

Substituting into Eq. (20) then gives

$$B = \frac{m^2}{\mu^2} \frac{8\pi^2}{3H_0^4} \left[ U(\psi_+) - \frac{7(2-3\psi_+)}{120(1-\nu\psi_+)} (\omega^2 - 4H_0^2)^2 + \dots \right]. \quad (29)$$

For  $\nu = 0$  this gives

$$B = \frac{m^2}{\mu^2} \frac{4\pi^2}{81H_0^4} \left[ 1 - \frac{63}{20} (1 - 4H_0^2)^2 + \dots \right], \quad (30)$$

and for  $\nu = 1$  it gives

$$B = \frac{m^2}{\mu^2} \frac{\pi^2}{12H_0^4} \left[ 1 - \frac{7}{15} (1 - 8H_0^2)^2 + \dots \right]. \quad (31)$$

### 3.2 The thin-wall approximation

From Eqs. (10) and (12),

$$U(\psi) = \frac{1}{2}\psi^2(1-\psi)^2 - \frac{1}{2}\varepsilon\psi^4. \quad (32)$$

In the thin-wall approximation,  $\varepsilon \ll 1$  so that the true and false vacua are nearly degenerate, and  $H_0 \ll 1$  so that a large bubble can fit into the Euclidean de Sitter space. The instanton can then be divided into three regions

1. Inside the bubble where

$$\psi = \psi_- \simeq 1 \quad \text{and} \quad U \simeq -\frac{1}{2}\varepsilon. \quad (33)$$

2. The bubble wall where

$$\zeta \simeq \zeta_w, \quad \ddot{\psi} \simeq U' \quad \text{and} \quad U \simeq \frac{1}{2}\psi^2(1-\psi)^2. \quad (34)$$

Therefore

$$\dot{\psi} \simeq -\sqrt{2U} \simeq -\psi(1-\psi) \quad \left( \text{therefore} \quad \psi = \frac{1}{1 + e^{\zeta - \zeta_w}} \right). \quad (35)$$

3. Outside the bubble where

$$\psi = 0. \quad (36)$$

Putting it all into Eq. (20) then gives

$$B = \frac{m^2 2\pi^2}{\mu^2 H_0^3} \left[ -\frac{1}{2}\varepsilon \int_0^{\zeta_W} d\zeta \sin^3 H_0\zeta + \sin^3 H_0\zeta_W \int_0^1 d\psi \psi(1-\psi) \right], \quad (37)$$

$$= \frac{m^2 2\pi^2}{\mu^2 H_0^3} \left[ -\frac{1}{2} \frac{\varepsilon}{H_0} \left( \frac{2}{3} - \cos H_0\zeta_W + \frac{1}{3} \cos^3 H_0\zeta_W \right) + \frac{1}{6} \sin^3 H_0\zeta_W \right], \quad (38)$$

and maximising  $B$  with respect to  $\zeta_W$  gives

$$\tan H_0\zeta_W = \frac{H_0}{\varepsilon}. \quad (39)$$

Note that  $\rho_W = (1/H_0) \sin H_0\zeta_W = 1/\sqrt{\varepsilon^2 + H_0^2} \gg 1$ . Substituting back into  $B$  gives

$$B = \frac{m^2 \pi^2}{\mu^2 3} \frac{1}{\sqrt{\varepsilon^2 + H_0^2} \left( \varepsilon + \sqrt{\varepsilon^2 + H_0^2} \right)^2}. \quad (40)$$

Now we will calculate the first-order corrections in  $\varepsilon$  and  $H_0$  to Eq. (40). As before, divide the instanton into three parts.

1. Inside the bubble where

$$\psi = \psi_- \simeq 1 + 2\varepsilon \quad \text{and} \quad U \simeq -\frac{1}{2}\varepsilon(1 + 4\varepsilon). \quad (41)$$

2. The bubble wall where, from Eqs. (19), (35), and (39),

$$\ddot{\psi} \simeq U' - 3\varepsilon\dot{\psi} \simeq U' + 3\varepsilon\psi(1-\psi). \quad (42)$$

Therefore

$$\dot{\psi} \simeq -\left(1 - \frac{1}{2}\varepsilon\right)\psi(1-\psi) - 2\varepsilon\psi, \quad (43)$$

and

$$\frac{1}{2}\dot{\psi}^2 + U \simeq (1-\varepsilon)\psi^2(1-\psi)^2 + \frac{1}{2}\varepsilon\psi^2(5-6\psi). \quad (44)$$

Therefore  $\dot{\psi}^2/2 + U = O(\varepsilon^2)$  when  $\psi = O(\varepsilon)$  and  $\dot{\psi}^2/2 + U = -\varepsilon/2 + O(\varepsilon^2)$  when  $\psi = 1 + O(\varepsilon)$ . Therefore from Eq. (35) the boundaries of the bubble wall can be taken to be at  $\zeta = \zeta_W \pm \ln \varepsilon$ .

3. Outside the bubble where

$$\psi = 0. \quad (45)$$

Putting it all into Eq. (20) then gives

$$B = \frac{m^2 2\pi^2}{\mu^2 H_0^3} \left\{ -\frac{1}{2}\varepsilon(1+4\varepsilon) \int_0^{\zeta_W + \ln \varepsilon} d\zeta \sin^3 H_0\zeta + \int_{\zeta_W + \ln \varepsilon}^{\zeta_W - \ln \varepsilon} d\zeta \sin^3 H_0\zeta \left[ (1-\varepsilon)\psi^2(1-\psi)^2 + \frac{1}{2}\varepsilon\psi^2(5-6\psi) \right] \right\}, \quad (46)$$



which from Eqs. (35) and (43), and after noting that we can use Eq. (39) because  $\partial B/\partial\zeta_{\text{W}} = 0$ , eventually gives

$$B = \frac{m^2 \pi^2}{\mu^2} \frac{1}{3 \sqrt{\varepsilon^2 + H_0^2} \left( \varepsilon + \sqrt{\varepsilon^2 + H_0^2} \right)^2} \left[ 1 + \frac{11}{2} \varepsilon + \frac{3\varepsilon^2}{\sqrt{\varepsilon^2 + H_0^2}} + \frac{3\varepsilon^3}{2(\varepsilon^2 + H_0^2)} \right]. \quad (47)$$

In the limit,  $H_0 \ll \varepsilon$ , this gives

$$B = \frac{m^2 \pi^2}{\mu^2} \frac{\pi^2}{12\varepsilon^3} \left( 1 + 10\varepsilon - \frac{H_0^2}{\varepsilon^2} + \dots \right), \quad (48)$$

while in the limit  $\varepsilon \ll H_0$  it gives

$$B = \frac{m^2 \pi^2}{\mu^2} \frac{\pi^2}{3H_0^3} \left( 1 - 2\frac{\varepsilon}{H_0} + \dots \right), \quad (49)$$

so that we need to calculate to a higher order in  $H_0$  in this limit to get the first-order correction. We will now do this.

Set  $\varepsilon = 0$ . Then

$$U = \frac{1}{2} \psi^2 (1 - \psi)^2, \quad (50)$$

and by symmetry  $\zeta_{\text{W}} = \pi/2H_0$ . Therefore, from Eq. (19),

$$\begin{aligned} \dot{\psi}^2 &= 2U - 6H_0 \int d\zeta \cot H_0 \zeta \dot{\psi}^2, \\ &= 2U \left[ 1 + O(H_0^2) \right]. \end{aligned} \quad (51)$$

Therefore

$$\frac{\frac{1}{2} \dot{\psi}^2 + U}{\dot{\psi}} = -\sqrt{2U} \left[ 1 + O(H_0^4) \right]. \quad (52)$$

Therefore from Eqs. (20) and (35),

$$\begin{aligned} B &= \frac{m^2}{\mu^2} \frac{2\pi^2}{H_0^3} \int_0^1 d\psi \left[ 1 - \frac{3}{2} H_0^2 \ln^2 \left( \frac{1}{\psi} - 1 \right) \right] \psi(1 - \psi) + \dots, \\ &= \frac{m^2 \pi^2}{\mu^2} \frac{\pi^2}{3H_0^3} \left[ 1 - \frac{1}{2} (\pi^2 - 6) H_0^2 + \dots \right]. \end{aligned} \quad (53)$$

## 4 Numerical Results

We solved Eq. (19) numerically with  $\nu$  and  $H_0$  taking values in the parameter space shown in Figure 1, and calculated the corresponding values of  $\tilde{B}$ , which is defined by

$$B = \frac{m^2 \pi^2}{12\mu^2} \tilde{B}. \quad (54)$$

The results, with the thin-wall divergence, Eq. (40), factored out, are plotted in Figure 2. We then fitted various analytic formulae to the results, first for the special cases of the straight boundaries of the parameter space and then for the full two-dimensional case.

## 4.1 One-dimensional fitting

### $\nu = 0$ : a cubic potential

We obtained  $\tilde{B} = 27.62$  in the  $\nu = H_0 = 0$  limit with the accuracy to the given figures, and, from Eq. (30),  $\tilde{B} = 256/27$  in the Hawking-Moss limit ( $H_0 = 1/2$ ). We compared the numerically calculated  $\tilde{B}$  with

$$\tilde{B}_{\text{fit}} = 27.62 - 72.55H_0^2, \quad (55)$$

where the coefficients were chosen to give an exact fit at both boundaries of the parameter region. In this case the relative error  $(\tilde{B} - \tilde{B}_{\text{fit}})/\tilde{B}$  is found to be  $< 0.6\%$ . A more accurate fit, again exact at both boundaries, is given by

$$\tilde{B} = 27.62 - 71.02H_0^2 - 24.48H_0^6. \quad (56)$$

Now the relative error becomes  $< 2.6 \times 10^{-4}$ .

### $\varepsilon = 0$ : degenerate vacua

The numerical results for this case have already been obtained in Ref. [2] and applied to the nucleation of spherical domain-wall bubbles during inflation. From Eq. (53) we can see that  $\tilde{B} \rightarrow 4/H_0^3$  as  $H_0 \rightarrow 0$ . Also, from Eq. (31), we get  $\tilde{B} = 64$  in the Hawking-Moss limit ( $H_0 = 1/\sqrt{8}$ ). Thus the simplest fitting exact at both boundaries is

$$\tilde{B} = \frac{4}{H_0^3} \left[ 1 - 8 \left( 1 - \frac{1}{\sqrt{2}} \right) H_0^2 \right], \quad (57)$$

with a relative error  $< 2\%$ . A better fit, again exact at both boundaries, is given by

$$\tilde{B} = \frac{4}{H_0^3} \left[ 1 - 1.887H_0^2 - 3.649H_0^4 \right]. \quad (58)$$

In this case, the relative error is  $< 6 \times 10^{-4}$ .

### $H_0 = 0$ : flat space

This case has already been examined in [7]. In our notation, his results are

$$\tilde{B} = \frac{1}{\varepsilon^3} \left( 1 + a\varepsilon + b\varepsilon^2 \right), \quad (59)$$

with

$$a = 10.052 \quad \text{and} \quad b = 16.612. \quad (60)$$

This fitting formula is not insufficient but it has its largest relative error ( $\sim 0.17\%$ ) at  $\nu = 0$ . However, the choice of parameters

$$a = 10.07 \quad \text{and} \quad b = 16.55, \quad (61)$$

is better, making the fitting exact at both boundaries, and giving a relative error  $< 0.14\%$ .

## 4.2 Two-dimensional fitting

Now we try to give a fitting formula valid in the whole range of parameter space. Looking at the rather complicated form of Eq. (47), we can guess that it is not easy to obtain a simple fitting formula. Figures 3(a) and 3(b) are plots of  $\tilde{B}_1$  and  $\tilde{B}_2$  which are defined by

$$\tilde{B} = \frac{4(1 + 10.07\varepsilon + 16.55\varepsilon^2)}{\delta(\varepsilon + \delta)^2} \tilde{B}_1, \quad (62)$$

$$= \frac{4(1 + 10.07\varepsilon + 16.55\varepsilon^2)}{\delta(\varepsilon + \delta)^2(1 + 10\varepsilon)} \left[ 1 + \frac{11}{2}\varepsilon + 3\frac{\varepsilon^2}{\delta} + \frac{3\varepsilon^3}{2\delta^2} \right] \tilde{B}_2, \quad (63)$$

where  $\delta \equiv \sqrt{\varepsilon^2 + H_0^2}$ . From these plots, it seems better to try to fit  $\tilde{B}_2$  instead of  $\tilde{B}$  or  $\tilde{B}_1$ , despite its more complicated factor. Since this factor is written in terms of  $\varepsilon$  and  $\delta$ , we try to fit  $\tilde{B}_2$  with a polynomial of these two parameters. To keep the relative error less than about 1%, at least ten terms seem to be necessary. We give one example of the fitting:

$$\tilde{B}_2 = 1 + \sum_{ij} a_{ij} \varepsilon^i \delta^j, \quad (64)$$

with nonzero coefficients

$$\begin{aligned} a_{01} &= -0.1617, & a_{03} &= -5.507, \\ a_{11} &= -11.34, & a_{12} &= 30.17, & a_{14} &= -21.69, \\ a_{20} &= 12.09, & a_{21} &= -33.24, & a_{23} &= 41.29, \\ a_{30} &= 7.728, & \text{and} & & a_{32} &= -19.34. \end{aligned} \quad (65)$$

Factoring out the complicated thin-wall factor was necessary to remove the divergence in the thin-wall limit. Therefore, for small  $\nu$ ,  $\tilde{B}$  is expected to be fitted by a simpler formula. We give the following example of a fitting for  $\nu \leq 0.4$ :

$$\tilde{B} = \frac{1}{\varepsilon^3} \left( 1 + 10.07\varepsilon + 16.55\varepsilon^2 \right) \left[ \frac{1 + (a + b\nu)H_0^2}{1 + (c + d\nu + e\nu^2)\nu^2 H_0^2} \right], \quad (66)$$

with

$$a = -2.635, \quad b = -0.378, \quad c = 43.6, \quad d = -130, \quad \text{and} \quad e = 163. \quad (67)$$

The relative error of this fitting is  $< 1.4\%$ .

## 5 Conclusions

We have thoroughly investigated the tunneling rate for a scalar field with a general quartic potential in de Sitter space in the limit of no gravitational back reaction. In this case, the number of parameters of the theory essentially reduces to two. We have numerically calculated the tunneling rates over this two-dimensional parameter space. Based on analytic formulae which are valid for extreme values of the parameters, we have constructed approximate formulae from the numerical results with relative errors of  $\lesssim 1\%$ . Since these approximate formulae incorporate the effect of the background curvature, they have a wider range of applicability than previously known formulae. Hence our results will provide a better understanding of quantum tunneling phenomena and the associated physical processes in the early Universe.

## Acknowledgements

EDS is supported by a JSPS Postdoctoral Fellowship and TT is supported by a JSPS Junior Scientist Fellowship. This work was supported by Monbusho Grant-in-Aid for Encouragement of Young Scientists Nos. 2010 and 92062, Monbusho Grant-in-Aid for Scientific Research No. 05640342, and the Sumitomo Foundation.

## References

- [1] D. La and P. J. Steinhardt, Phys. Rev. Lett. **62**, 376 (1989);  
P. J. Steinhardt and F. S. Accetta, Phys. Rev. Lett. **64**, 2740 (1990);  
F. C. Adams and K. Freese, Phys. Rev. D **43**, 353 (1991);  
R. Holman, E. W. Kolb, S. L. Vadas and Y. Wang, Phys. Lett. **B269**, 252 (1991);  
A. R. Liddle and D. Wands, Phys. Rev. D **45**, 2662 (1992);  
E. J. Copeland, A. R. Liddle, D. H. Lyth, E. D. Stewart and D. Wands, to appear, Phys. Rev. D (1994).
- [2] R. Basu, A. H. Guth and A. Vilenkin, Phys. Rev. D **44**, 340 (1991);  
R. Basu and A. Vilenkin, Phys. Rev. D **46**, 2345 (1992).
- [3] M. B. Voloshin, I. Yu. Kobzarev and L. B. Okun, Yad. Fiz. **20**, 1229 (1974) [Sov. J. Nucl. Phys. **20**, 644 (1975)].

- [4] S. Coleman, Phys. Rev. D **15**, 2929 (1977);  
C. G. Callan and S. Coleman, Phys. Rev. D **16**, 1762 (1977).
- [5] S. Coleman and F. De Luccia, Phys. Rev. D **21**, 3305 (1980).
- [6] S. W. Hawking and I. G. Moss, Phys. Lett. **B110**, 35 (1982).
- [7] F. C. Adams, Phys. Rev. D **48**, 2800 (1993).
- [8] S. Coleman, *Aspects of Symmetry* (Cambridge University Press, Cambridge, 1985).
- [9] S. Coleman, V. Glaser and A. Martin, Commun. Math. Phys. **58**, 211 (1978).
- [10] S. Parke, Phys. Lett. **B121**, 313 (1983).
- [11] L. G. Jensen and P. J. Steinhardt, Nucl. Phys. **B237**, 176 (1984).
- [12] T. Tanaka and M. Sasaki, Prog. Theor. Phys. **88**, 503 (1992).

## Figure Captions

### Figure 1: Parameter space

The dotted line (given by Eq. (25)) marks the boundary between the regions where the Hawking-Moss (HM) instanton (see Section 3.1) and our numerically calculated instantons dominate. The corner labeled TW is where the thin-wall approximation (see Section 3.2) is valid. The boundaries labeled CP, FS, and DV correspond to the limits of a cubic potential, flat space, and degenerate vacua, respectively (see Section 4.1). The solid lines are a contour plot of our numerical results (and of the analytic results in the Hawking-Moss region).  $\tilde{B}$  is defined in Eq. (54).

### Figure 2: Numerical results

The numerical results expressed in terms of  $B/B_{\text{TW}}$ , where  $B_{\text{TW}}$  is the thin-wall bounce action given in Eq. (40).

### Figure 3

A comparison of two possible choices of functions to be fitted by analytic formulae.  $\tilde{B}_1$  and  $\tilde{B}_2$  are defined in Eqs. (62) and (63), respectively.

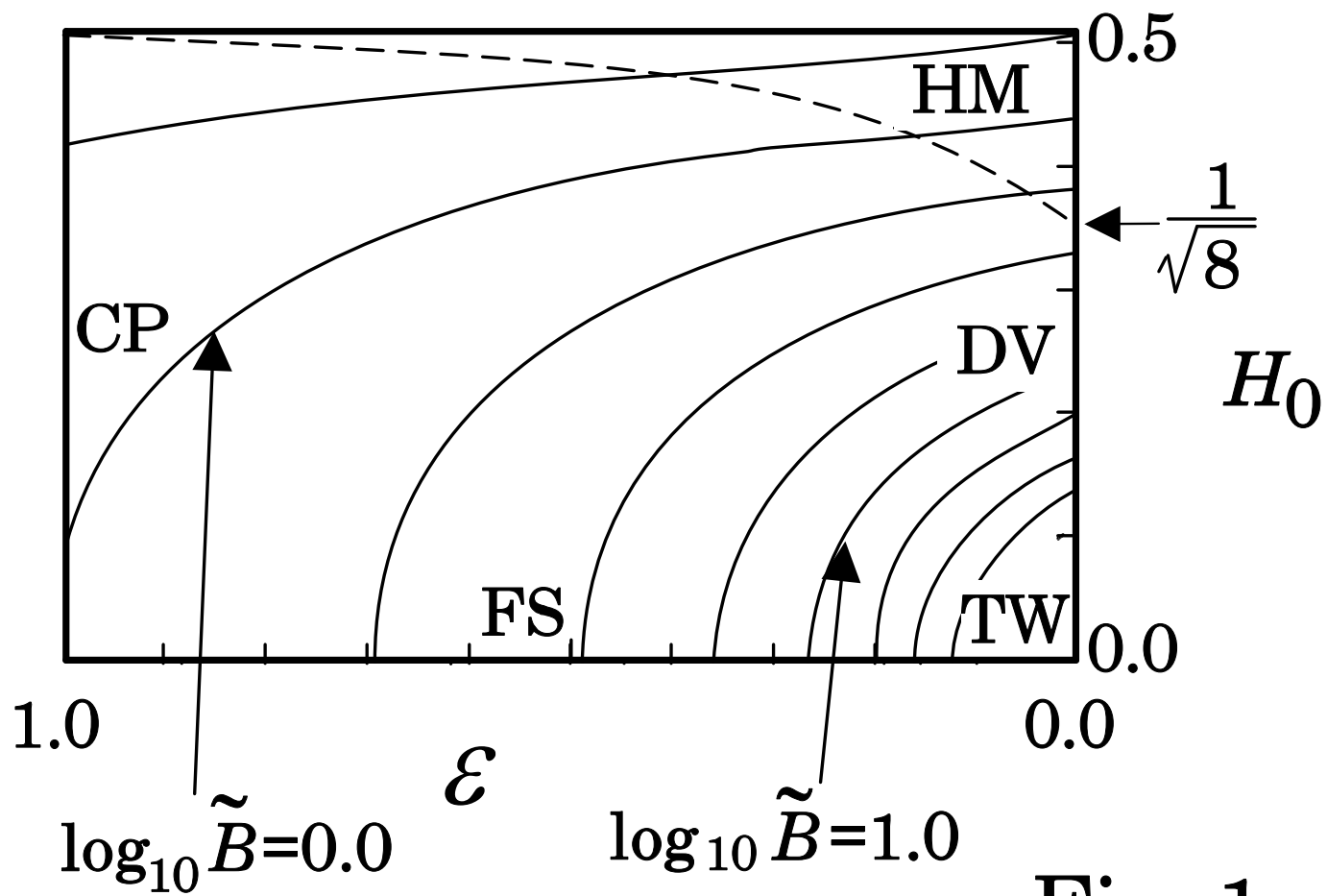


Fig. 1

This figure "fig1-1.png" is available in "png" format from:

<http://arxiv.org/ps/hep-ph/9402247v2>

This figure "fig2-1.png" is available in "png" format from:

<http://arxiv.org/ps/hep-ph/9402247v2>



This figure "fig3-1.png" is available in "png" format from:

<http://arxiv.org/ps/hep-ph/9402247v2>

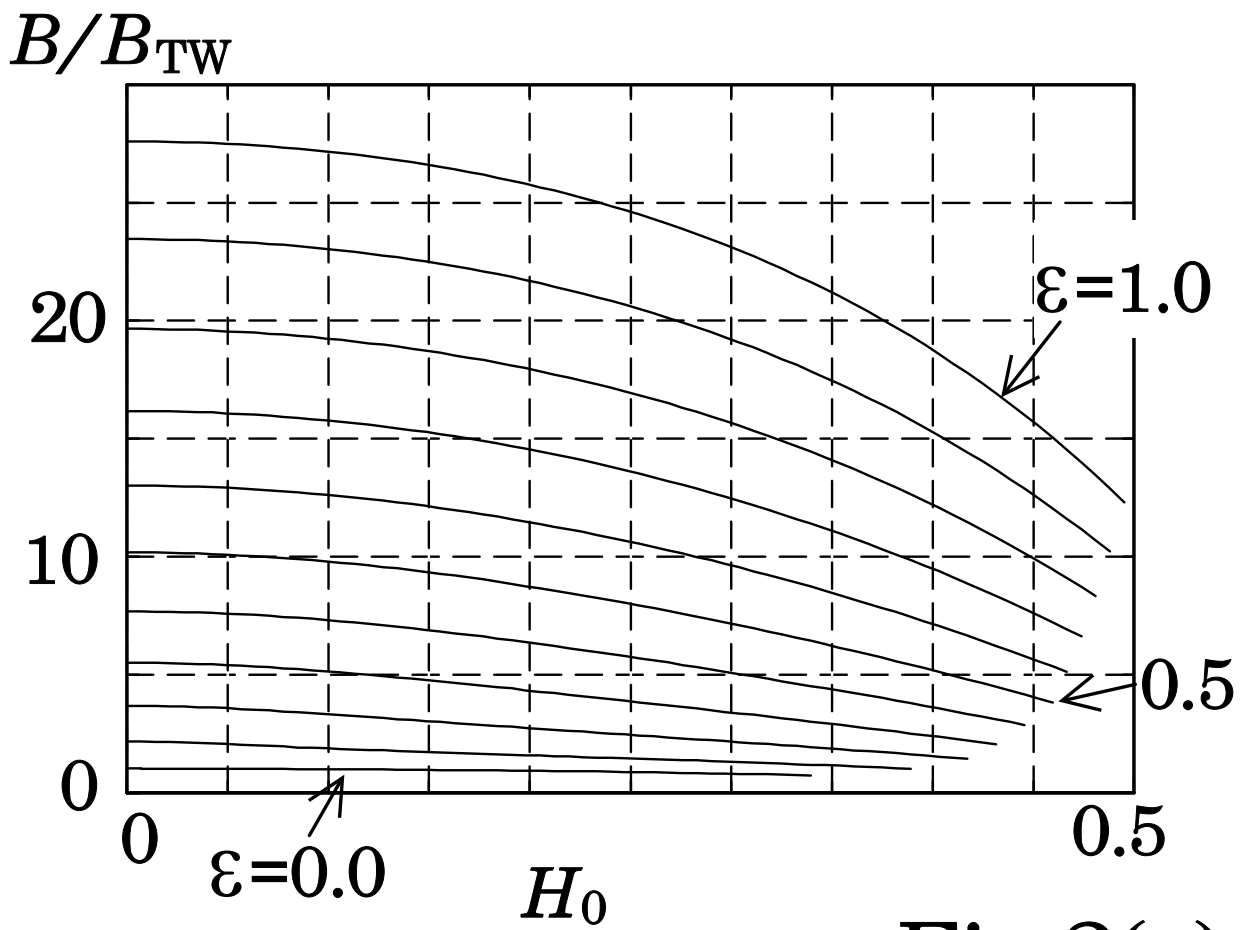


**Fig.2(a)**

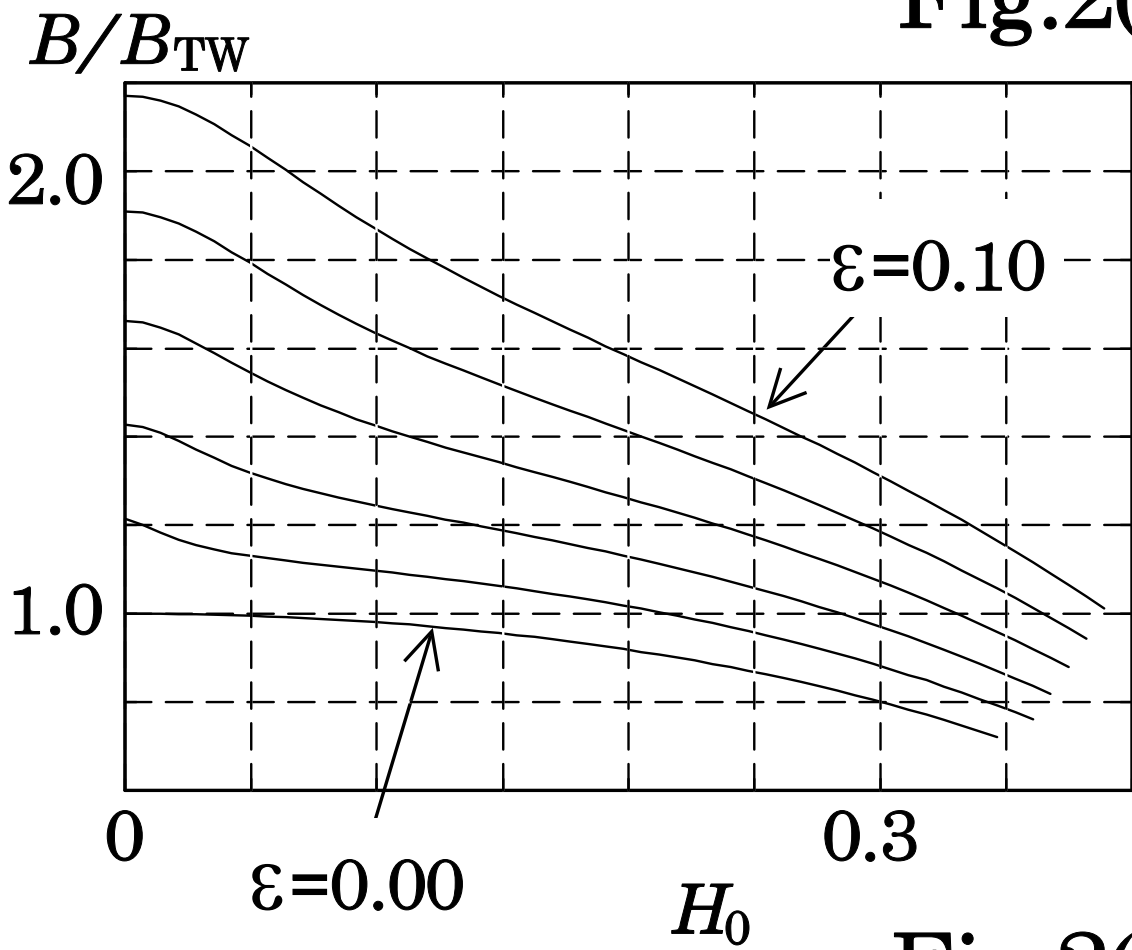


**Fig.2(b)**

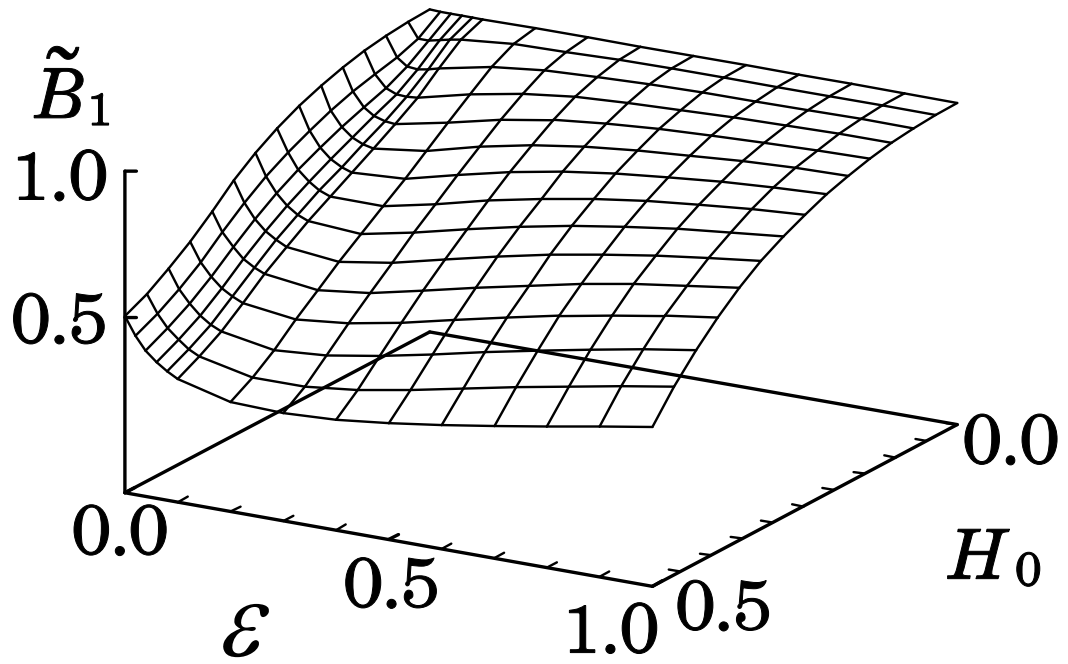


Fig.3(a)

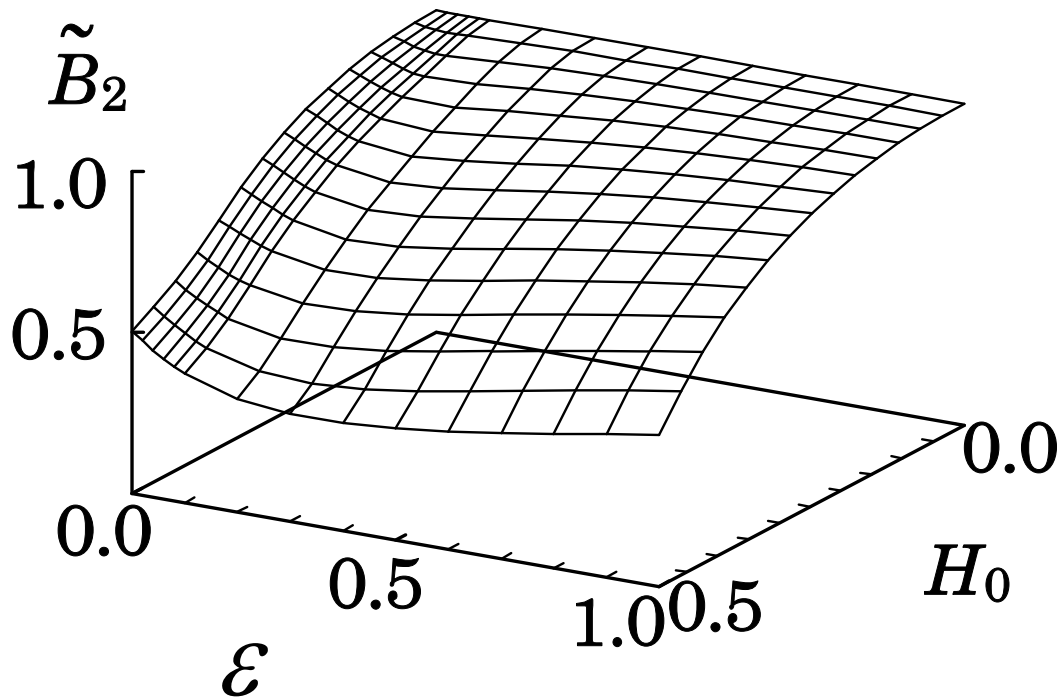


Fig.3(b)